



# Optimal strain gage location for determination of mode I stress intensity factor for orthotropic laminates using a single strain gage

Debabrata Chakraborty\*, Debaleena Chakraborty, K. S. R. Krishna Murthy

Department of Mechanical Engineering, Indian Institute of Technology Guwahati, Guwahati 781039, India

## ABSTRACT

The present work discusses a robust method developed for determination of mode I stress intensity factor ( $K_I$ ) of orthotropic laminates using a single strain gage and based on a three parameter strain series representation ahead of the crack tip. Appropriate radial location of the strain gage ahead of the crack tip is important in the sense that strain gages placed either very near or very far from the crack tip might lead to inaccuracies in the estimated SIFs due to 3D effects near the crack tip or inaccurate strain field representation at farther distances. The theoretical formulation has been presented for determination of angular location, orientation and the upper bound on the radial location ( $r_{\max}$ ) for pasting the strain gage which could be subsequently used for accurate determination of  $K_I$ . Numerical simulations have been presented considering edge cracked  $[90_2/0]_{10S}$  carbon-epoxy orthotropic laminates to illustrate the determination of  $r_{\max}$  and  $K_I$  of such laminates.

## ARTICLE INFO

### Article history:

Received 21 August 2016

Accepted 24 September 2016

### Keywords:

Orthotropic

Stress intensity factor

Strain gage

Gage location

Radial location

## 1. Introduction

Fracture mechanics analyses of composite materials is essential due to the increasing use of these materials in many engineering applications. The concepts of linear elastic fracture mechanics (LEFM) of relevance to isotropic materials have also been employed to composite materials after incorporating suitable provision to take care of the directional properties of such materials, the pioneering works towards which was started off by Irwin (1962) and Wu (1963). The effective application of LEFM in predicting and preventing fracture lies in the availability of accurate values of SIF, which is a LEFM parameter that decides whether an existing crack in a component grows or not. Experimental determination of SIFs of cracked composite panels has raised substantial interest not only in complex situations but also to validate the numerical and analytical results. Among the experimental techniques, the simplest and least expensive is the method of SIF determination using strain gages.

In case of isotropic materials, a single strain gage technique proposed by Dally and Sanford (1987) was the first practical and feasible approach towards determination of

mode I SIF ( $K_I$ ) of plane problems. The Dally and Sanford technique or popularly the DS technique is based on a three parameter representation of the strain field around the crack tip and necessitates a single strain gage oriented along a certain angle,  $\phi$  and placed at a location decided by the angle,  $\theta$  as shown in Fig. 1. The radial distance of the strain gage with respect to the crack tip also plays a very crucial role in ensuring the accuracy of the SIFs estimated using strain gages. Strain gages placed either very near or very far from the crack tip might lead to inaccuracies in the estimated SIFs due to 3D effects, strain gradients near the crack tip or inaccurate strain field representation at farther distances. This issue was addressed for the first time by Sarangi and co-workers for isotropic materials (2010). They proposed a methodology to estimate the optimal location of a strain gage in association with the DS technique.

For orthotropic materials, only recently Chakraborty et al. (2014) presented an extension of the DS technique in entirety for determination of  $K_I$ . Suggestions for optimal gage locations were also proposed employing a finite element based approach supported with proper theoretical formulations. Using the same technique, an

\* Corresponding author. Tel.: +91-361-2582666; Fax: +91-361-2582699; E-mail address: chakra@iitg.ernet.in (D. Chakraborty)

attempt has been made in the present work to determine ( $K_I$ ) of  $[90_2/0]_{10S}$  Carbon-epoxy laminates having an edge-cracked configuration using numerical simulations. In addition, the influence of optimal gage locations on the accuracy of the estimated SIFs has also been studied using numerical analysis.

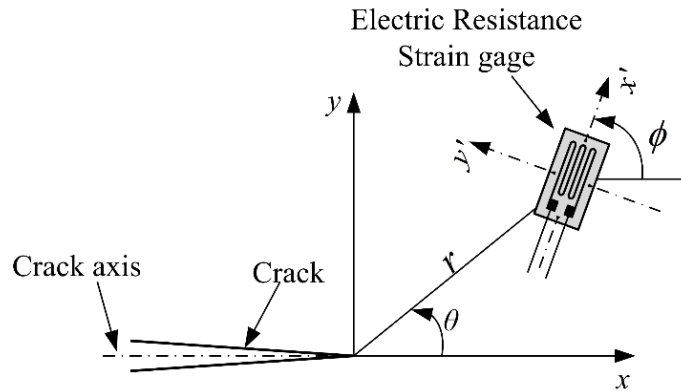


Fig. 1. Location of a strain gage.

2. Theoretical Background

The single strain gage technique that has been developed for the determination of  $K_I$  of orthotropic materials as an extension of the DS technique is presented here. Furthermore, the theoretical framework for estimating the optimal gage location has also been shown. For orthotropic materials, the normal strain component at a point  $P(r, \theta)$  along  $\phi$  (refer Fig. 1) for plane stress conditions, taking into account a three parameter strain series representation can be written as

$$\begin{aligned} \epsilon_{x'x'} = A_0 & \left\{ \left[ \frac{1}{\sqrt{r_1}} \left( \cos \frac{\theta_1}{2} \frac{\alpha - \beta}{2\alpha} \left( \cos^2 \phi (-\alpha_{11}(\alpha + \beta)^2 + \alpha_{12}) + \sin^2 \phi (-\alpha_{12}(\alpha + \beta)^2 + \alpha_{22}) \right) - \left( \sin \frac{\theta_1}{2} a_{66} \sin \phi \cos \phi \left( \frac{\alpha^2 - \beta^2}{2\alpha} \right) \right) \right] \right\} \\ & + \left\{ \left[ \frac{1}{\sqrt{r_2}} \left( \cos \frac{\theta_2}{2} \frac{\alpha - \beta}{2\alpha} \left( \cos^2 \phi (-\alpha_{11}(\alpha + \beta)^2 + \alpha_{12}) + \sin^2 \phi (-\alpha_{12}(\alpha + \beta)^2 + \alpha_{22}) \right) + \left( \sin \frac{\theta_2}{2} a_{66} \sin \phi \cos \phi \left( \frac{\alpha^2 - \beta^2}{2\alpha} \right) \right) \right] \right\} \\ & + A_1 \left\{ \left[ \sqrt{r_1} \left( \cos \frac{\theta_1}{2} \frac{\alpha - \beta}{2\alpha} \left( \cos^2 \phi (-\alpha_{11}(\alpha + \beta)^2 + \alpha_{12}) + \sin^2 \phi (-\alpha_{12}(\alpha + \beta)^2 + \alpha_{22}) \right) + \left( \sin \frac{\theta_1}{2} a_{66} \sin \phi \cos \phi \left( \frac{\alpha^2 - \beta^2}{2\alpha} \right) \right) \right] \right\} \\ & + \left\{ \left[ \sqrt{r_2} \left( \cos \frac{\theta_2}{2} \frac{\alpha - \beta}{2\alpha} \left( \cos^2 \phi (-\alpha_{11}(\alpha + \beta)^2 + \alpha_{12}) + \sin^2 \phi (-\alpha_{12}(\alpha + \beta)^2 + \alpha_{22}) \right) - \left( \sin \frac{\theta_2}{2} a_{66} \sin \phi \cos \phi \left( \frac{\alpha^2 - \beta^2}{2\alpha} \right) \right) \right] \right\} \\ & + B_0 \left\{ \frac{\beta}{2\alpha} [(\alpha + \beta)^2 - (\beta - \alpha)^2] (a_{11} \cos^2 \phi + a_{12} \sin^2 \phi) \right\}, \end{aligned} \tag{1}$$

where,

$$a_{11} = 1/E_L, \quad a_{12} = -\nu_{LT}/E_L = -\nu_{TL}/E_T, \quad a_{66} = 1/G_{LT}, \quad 2\beta^2 = \frac{a_{66} + 2a_{12}}{2a_{11}} + \sqrt{\frac{a_{22}}{a_{11}}}, \quad 2\alpha^2 = \frac{a_{66} + 2a_{12}}{2a_{11}} - \sqrt{\frac{a_{22}}{a_{11}}}, \tag{2}$$

and

$$\begin{aligned} \tan \theta_1 &= (\beta + \alpha) \tan \theta, \quad \tan \theta_2 = (\beta - \alpha) \tan \theta, \\ r_1^2 &= r^2 (\cos^2 \theta + (\beta + \alpha)^2 \sin^2 \theta), \quad r_2^2 = r^2 (\cos^2 \theta + (\beta - \alpha)^2 \sin^2 \theta). \end{aligned} \tag{3}$$

$L$  and  $T$  represent the longitudinal and transverse direction of the laminate (Fig. 1) and  $E, \nu$  and  $G$  represent Young’s modulus, Poisson’s ratio and shear modulus respectively. The specific values of  $\phi$  and  $\theta$  for which the coefficients of the terms containing  $A_1$  and  $B_0$  become zero are obtained as

$$\tan^2 \phi = -a_{11}/a_{12} = 1/v_{LT}, \tag{4}$$

and

$$\begin{aligned} & \sqrt[4]{(\cos^2 \theta + (\beta + \alpha)^2 \sin^2 \theta)} \left\{ \left[ \frac{1}{E_T} \left( \frac{1-v_{LT}v_{TL}}{1+v_{LT}} \right) \frac{\alpha-\beta}{2\alpha} \cos \left( \frac{1}{2} (\tan^{-1}((\beta + \alpha) \tan \theta)) \right) \right] \right\} + \\ & \sqrt[4]{(\cos^2 \theta + (\beta - \alpha)^2 \sin^2 \theta)} \left\{ - \left[ \frac{1}{G_{LT}} \left( \frac{v_{LT}}{(1+v_{LT})\sqrt{v_{LT}}} \right) \frac{1}{2\alpha} \sin \left( \frac{1}{2} (\tan^{-1}((\beta + \alpha) \tan \theta)) \right) \right] \right\} + \\ & \sqrt[4]{(\cos^2 \theta + (\beta - \alpha)^2 \sin^2 \theta)} \left\{ \left[ \frac{1}{E_T} \left( \frac{1-v_{LT}v_{TL}}{1+v_{LT}} \right) \frac{\alpha-\beta}{2\alpha} \cos \left( \frac{1}{2} (\tan^{-1}((\beta - \alpha) \tan \theta)) \right) \right] \right\} + \\ & \sqrt[4]{(\cos^2 \theta + (\beta - \alpha)^2 \sin^2 \theta)} \left\{ + \left[ \frac{1}{G_{LT}} \left( \frac{v_{LT}}{(1+v_{LT})\sqrt{v_{LT}}} \right) \frac{1}{2\alpha} \sin \left( \frac{1}{2} (\tan^{-1}((\beta - \alpha) \tan \theta)) \right) \right] \right\} = 0, \end{aligned} \tag{5}$$

respectively. Therefore, Eq. (1) may be rewritten using these values of  $\theta$  and  $\phi$  as

$$\varepsilon_{x'x'} = \frac{1}{\sqrt{r}} \times A_0 \left\{ \begin{aligned} & \left[ \frac{1}{E_T} \left( \frac{1-v_{LT}v_{TL}}{1+v_{LT}} \right) \frac{1}{2\alpha} \left[ \frac{\cos(\frac{1}{2} \tan^{-1}((\beta+\alpha) \tan \theta))}{\sqrt[4]{(\cos^2 \theta + (\beta+\alpha)^2 \sin^2 \theta)}} (\alpha - \beta) + \frac{\cos(\frac{1}{2} \tan^{-1}((\beta-\alpha) \tan \theta))}{\sqrt[4]{(\cos^2 \theta + (\beta-\alpha)^2 \sin^2 \theta)}} (\alpha + \beta) \right] \right] \\ & + \frac{1}{G_{LT}} \left\{ \frac{v_{LT}}{(1+v_{LT})\sqrt{v_{LT}}} \right\} \frac{1}{2\alpha} \left[ \frac{\sin[\frac{1}{2} \tan^{-1}\{(\beta+\alpha) \tan \theta\}]}{\sqrt[4]{(\cos^2 \theta + (\beta+\alpha)^2 \sin^2 \theta)}} - \frac{\sin[\frac{1}{2} \tan^{-1}\{(\beta-\alpha) \tan \theta\}]}{\sqrt[4]{(\cos^2 \theta + (\beta-\alpha)^2 \sin^2 \theta)}} \right] \right\} \end{aligned} \right\} = \frac{A_0}{\sqrt{r}} \times C = \frac{C'}{\sqrt{r}}, \tag{6}$$

where  $C$  is a constant for a given value of  $\theta$ ,  $\phi$  and material properties. From standard definition, the mode I SIF, ( $K_I$ ) can be obtained from the coefficient  $A_0$  as

$$K_I = \sqrt{2\pi} A_0. \tag{7}$$

Now, taking logarithm on both sides of Eq. (6) we get

$$\ln(\varepsilon_{x'x'}) = -\frac{1}{2} \ln(r) + \ln(C'). \tag{8}$$

Eq. (8) represents a straight line between  $\ln(\varepsilon_{x'x'})$  and  $\ln(r)$  with a slope of -0.5 and an intercept of  $\ln(C')$ . The straight line property remains up to a certain radial location from the crack tip ( $r_{max}$ ) and deviates beyond that as more than three parameters would be needed in Eq. (1) to estimate the  $\varepsilon_{x'x'}$ . It has been reported earlier by Shukla et al. (1989) that for orthotropic materials 3D effects prevailed up to a radial distance equal the thickness of the plate from the crack tip. Therefore, the minimum radial distance ( $r_{min}$ ) for strain measurements on the free surface which are under plane stress conditions should be greater than the thickness of the plate. As a consequence, the optimal gage location for pasting a strain gage can be given as

$$r_{min} (= \text{thickness of plate, } t) \leq r \leq r_{max}. \tag{9}$$

Thus, by placing a single strain gage as shown in Fig. 1 oriented at an angle of  $\phi$  at a radial distance  $r$  within  $r_{max}$  from the crack tip along the gage line at an angle of  $\theta$ , the measured strain  $\varepsilon_{x'x'}$  can be used to obtain ( $K_I$ ) using Eqs. (6) and (7).

### 3. Numerical Simulations

An edge cracked [90<sub>2</sub>/0]<sub>10S</sub> carbon-epoxy laminate with  $b=100$  mm,  $a/b=0.4$ ,  $h/b=2$  and material properties as  $E_L=67.77$  GPa,  $E_T=142.7$  GPa,  $v_{LT}=0.01$ ,  $G_{LT}=4.304$  GPa subjected to uniform tensile stress ( $\sigma=100$  MPa) is considered (Fig. 2(a)). Following the procedure described in Section 2, the values of  $\phi$  and  $\theta$  for which the coefficients  $B_0$  and  $A_1$  become zero are found to be 84° and 61° respectively. Fig. 2(b) shows the analysis domain with boundary conditions used for the numerical analysis.

Finite element analysis is carried out using ANSYS 14 where, eight noded isoparametric elements (PLANE 183) have been used for finite element discretization of the plate and quarter point elements (QPE) have been used around the crack-tip to model the  $\sqrt{r}$  singularity.

Fig. 3(a) shows the typical finite element mesh considered after proper convergence study. The mesh has been designed such that the nodes of several elements are made to lie along the gage line which starts at the crack tip and terminates at the outer boundaries. According to the present technique, a single strain gage is to be placed at an appropriate location along the gage line and oriented along  $\phi$  within the estimated  $r_{max}$  for the configuration in order to measure the linear strain  $\varepsilon_{x'x'}$ .

From the finite element results, the linear strain  $\varepsilon_{x'x'}$  and radial distance ( $r$ ) are computed for all the nodes along the gage line. Fig. 3(b) gives the plot of  $\ln(\varepsilon_{x'x'})$  versus  $\ln(r)$  for all the nodal values along the gage line. Crack tip point is not plotted as the radius of this point is zero. It can be seen that the plot consists of a linear plot followed by a non-linear one as predicted by the theory.

The radial distance at which the plot changes from a linear to a non-linear one gives the value of  $r_{max}$  or the extent of the three parameter zone or the optimal radial location for the particular configuration for pasting the strain gage. A line of slope -0.5 is superposed on the plot of  $\ln(\epsilon_{x'x'})$  versus  $\ln(r)$  and considering this line to be

the exact solution, absolute percentage relative error at all values of radius of this plot is calculated. Finally,  $r_{max}$  is estimated as the radius at which the error is less than 1% (as one goes from right to left in Fig. 3(b)). The  $r_{max}$  for the configuration corresponding to the present problem is found to be 34 mm.

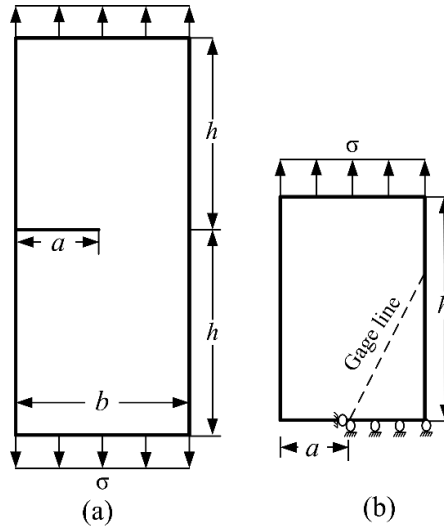


Fig. 2. (a) Orthotropic edge-cracked laminate; (b) Analysis domain for FEA.

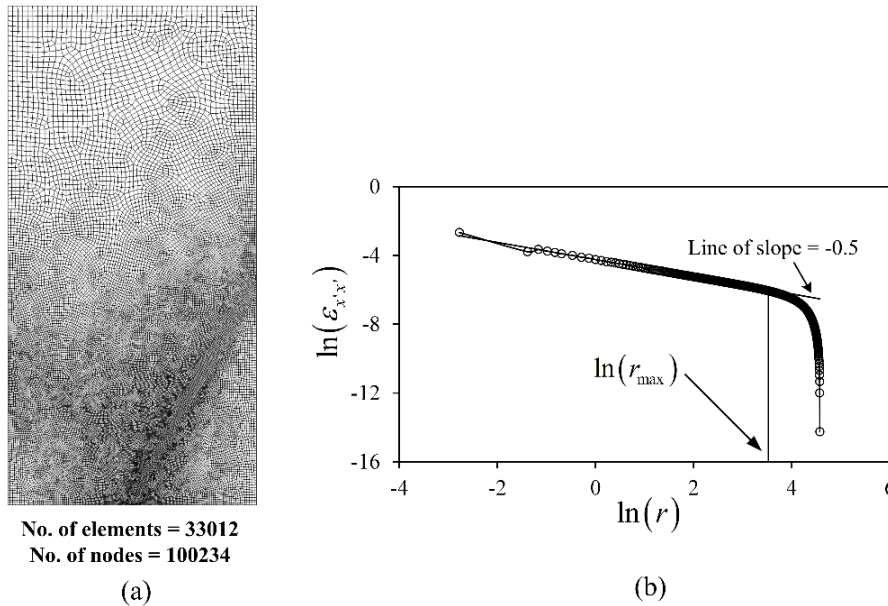


Fig. 3. (a) FE mesh of the laminate with  $a/b=0.5$ ; (b) Plot of  $\ln(\epsilon_{x'x'})$  vs.  $\ln(r)$  along the gage line.

The analytical value of mode I SIF of this configuration which will act as reference solution as per Tada et al. (2000) handbook is given by

$$K_I = Y_I(a/b)\sigma\sqrt{a}, \tag{10}$$

where  $\sigma$  is the applied stress,  $a$  is the crack length and  $Y_I$  is the specimen geometric factor given by

$$Y_I = 1.99 - 0.41(a/b)1.87(a/b)^2 - 38.48(a/b)^3 + 53.85(a/b)^4. \tag{11}$$

For this configuration with  $a/b$  of 0.5 and loaded at  $\sigma=100$  MPa the reference value of  $K_I$  is  $52.8 \text{ MPa}\sqrt{m}$ . Radial locations are selected within the optimal locations and outside the simulated  $r_{max}$  (non-optimal locations) to establish the importance of radial positioning of the strain gage. Measured  $K_I$  using Eqs. (6) and (7) from the strain readings at the selected radial locations are shown in Table 1. The percentage relative error in  $K_I$  measured at those locations is computed as

$$\% \text{ Rel. error} = \frac{K_{\text{reference solution}} - K_{\text{measured or simulated}}}{K_{\text{reference solution}}} \times 100. \tag{12}$$

Table 1 also enlists the computed relative error at the select radial locations. Results in Table 1 clearly show that it is possible to accurately determine  $K_I$  (error less than 2%) for an edge-cracked orthotropic laminate using a single strain gage if the gage is placed within  $r_{max}$ . On the other hand placing a strain gage outside  $r_{max}$  leads to

highly inaccurate values of  $K_I$ . These results substantiate that the present technique of determination of  $K_I$ . Using a single strain gage can be used for accurate determination of  $K_I$  for single ended cracked  $[90_2/0]_{10S}$  carbon-epoxy composite specimens if the gages are placed within the optimal locations.

**Table 1.**  $K_I$  of the edge cracked  $[90_2/0]_{10S}$  carbon-epoxy laminate at optimal and non-optimal positions.

$r$ (mm)	$r_{max} = 34$ mm	$\epsilon_{x'x'}$	$K_I$ (MPa $\sqrt{m}$ )	% Relative error
20.08	optimal	1.57E-03	53.04	0.45
25.18	optimal	1.38E-03	52.21	1.17
42.53	non-optimal	9.13E-04	44.89	14.98
50.19	non-optimal	7.11E-04	37.97	28.09

3.1. **Influence of  $a/b$  on  $r_{max}$**

In order to study the effect of  $a/b$  on  $r_{max}$ , edge cracked  $[90_2/0]_{10S}$  carbon-epoxy laminates with  $a/b$  ranging from 0.1 to 0.8 are considered, the other specifications of which including the material properties are same as that

have been used in the previous example. The plots of  $\ln(\epsilon_{x'x'})$  vs.  $\ln(r)$  for the nodes along the gage line for all the edge-cracked laminates are shown in Fig. 4(a). Following the procedure used in the previous example, the  $r_{max}$  value estimated for all the configurations is shown in Table 2.

**Table 2.** Variation of  $r_{max}$  with  $a/b$ .

$a/b$	$r_{max}$	$r_{max}/b$
0.1	4.5	0.045
0.2	7.8	0.078
0.3	15.5	0.155
0.4	34	0.34
0.5	67	0.67
0.6	19	0.19
0.7	10.9	0.109

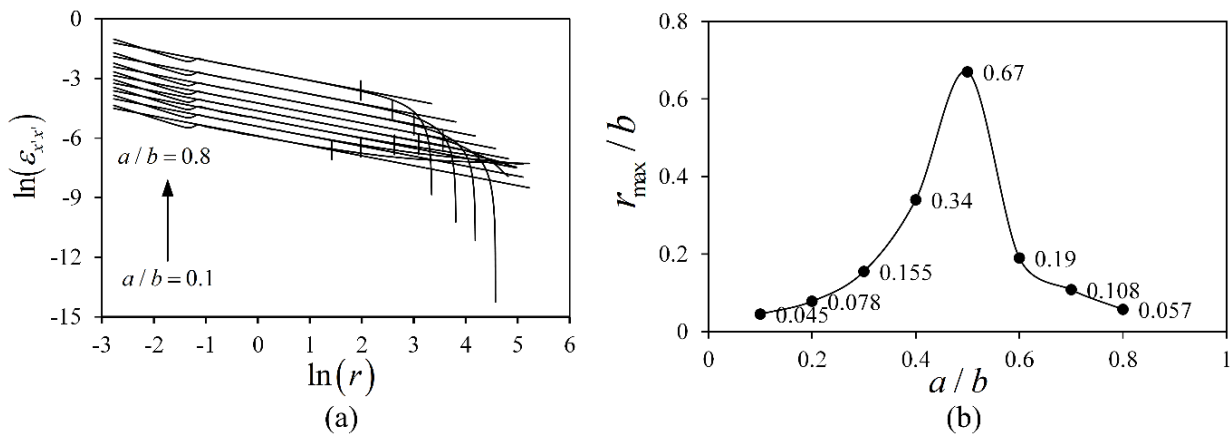


**Fig. 4.** (a)  $\ln(\epsilon_{x'x'})$  vs.  $\ln(r)$  with  $a/b = 0.1$  to  $0.8$ ; (b) Variation of  $r_{max}/b$  as a function of  $a/b$ .

Variation of non-dimensional  $r_{\max}/b$  as a function of  $a/b$  is shown in Fig. 4(b). It may be observed that the  $r_{\max}$  increases initially with increase in  $a/b$ , with a gradual decrease at higher values of  $a/b$ . This may be due to the fact that at low values of  $a/b$ , crack length in the controlling parameter for changes in  $r_{\max}$ . However, as the crack length increases, beyond a certain point, the boundary effects start having an impact on the  $r_{\max}$  as the gage line proceeds very near to the gage line.

#### 4. Conclusions

The single strain gage technique for the determination of mode I SIF of orthotropic laminates stands verified for the selected  $[90_2/0]_{10s}$  carbon-epoxy edge cracked laminates. Numerical simulations show that accurate values of  $K_I$  can be obtained only for strain gage readings within the optimal gage locations and  $K_I$  estimated for the numerically estimated strains at the non-optimal radial locations are erroneous. Furthermore, the optimal gage locations or  $r_{\max}$  is found to be dependent on both the crack length and the nearness to the boundary (boundary effects).

#### REFERENCES

- Chakraborty D, Murthy KSRR, Chakraborty D (2014). A new single strain gage technique for determination of mode I stress intensity factor in orthotropic composite materials. *Engineering Fracture Mechanics*, 124-125, 142-54.
- Dally JW, Sanford RJ (1987). Strain gage methods for measuring the opening mode stress intensity factor. *Experimental Mechanics*, 27, 381-388.
- Irwin GR (1962). Analytical aspects of crack stress field problems. T&AM Report No. 213, University of Illinois, Urbana.
- Sarangi H, Murthy KSRR, Chakraborty D (2010). Radial locations of strain gages for accurate measurement of mode I stress intensity factor. *Materials and Design*, 31, 2840–2850.
- Shukla A, Agarwal BD, Bhusan B (1989). Determination of stress intensity factor in orthotropic composite materials using strain gages. *Engineering Fracture Mechanics*, 32, 469-77.6.
- Tada H, Paris PC, Irwin GR (2000). The stress analysis of cracks handbook. ASME, New York.
- Wu EM (1963). On the application of fracture mechanics to orthotropic plates. T&AM Report No. 248, University of Illinois, Urbana.